European Journal of Soil Science, February 2005, **56,** 39–51 doi: 10.1111/j.1365-2389.2004.00638.x

Short-term effects of management on the soil structure in a deep tilled hardened volcanic-ash soil (cangahua) in Ecuador

P. PODWOJEWSKI[a] & N. GERMAIN[b]
[a]*IRD, IWMI, Ambassade de France, 57, Tran Hung Dao, Hanoi, Vietnam, and* [b]*IRD, 911, Avenue Agropolis, BP 64501, 34394 Montpellier Cedex, France*

Summary

In the Ecuadorian Cordillera, the hardened volcanic ashes (cangahuas) account for 15% of the cultivated area. The soil resulting from the fragmentation of these materials, generally by heavy machinery, shows an apparent stable millimetric structure. However, this new structure is highly susceptible to disintegration under rain, because it contains no organic matter and little clay, and the material itself is readily eroded in consequence.

We studied the evolution of soil aggregate stability in two factorial experiments during five cultivation cycles with two kinds of soil preparation and five fertilization treatments. The aggregate stability was not influenced by either kind of soil preparation, nor by large additions of cattle manure (80 t ha^{-1}) or green manure (10 t ha^{-1}), nor by growing a perennial grass. The variation in the aggregate stability seemed to depend on the components inherited from the original volcanic material: in the plots with larger clay content, and with swelling clay minerals, the aggregates were less stable than those composed of isometric fine silt particles.

Introduction

In several parts of highland tropical America there are beds of hard volcanic ash of late Pleistocene age at the surface or buried beneath a thin covering of loose ash. In Ecuador they are known as 'cangahua', and they occur mainly in the inter-Andean valley at altitudes of 2200–3000 m (Winckell & Zebrowski, 1992). Similar materials are referred to as 'tepetates' in Mexico and talpetates in Nicaragua (Quantin, 1992). They are increasingly being cultivated to feed growing populations, often with consequential erosion arising partly from the peculiarities of the material.

The hard cangahua is covered locally by a layer of loose sandy ash (up to 50 cm thick) of Holocene age. This ash has been eroded off where the hard material appears at the surface (De Noni *et al*., 2001). Figure 1 shows the typical appearance of the result. In some places, the hardened ash is covered with a thin layer (< 5 mm) of secondary calcrete or ferro-manganese concretions which seems to have been precipitated from water flowing at the interface of the hard ash and the loose cover.

The beds of cangahua of Ecuador are typically 50 cm or more thick, continuous, and with a massive structure. Like soil horizons, they lie approximately parallel to the land surface. They consist of acidic volcanic ash with the composition of rhyolite or dacite that has weathered somewhat. The material is hard and apparently weakly cemented, though the cementing agent has not been identified with any certainty.

The surface of the cangahua appears as tightly packed millimetric aggregates (Figure 2), which seem from their appearance to have formed by pedological processes. Weathering of isolated blocks of cangahua splits the blocks into two types of particles (Figure 3): (a) individual rounded particles from 0.2 to more than 1 cm in diameter which could be considered as weathered accretionary lapilli (Moore & Peck, 1962); and (b) angular fragments of very varied size but with an average diameter of 1–5 mm and which seem to be part of a matrix, including the lapilli. It seems that the deposition of the ash and lapilli was accompanied by heavy rain (Moore *et al*., 1966), so that the material formed a water-saturated mud that hardened with more or less cementation as it dried (Fischer & Schmincke, 1984). It softens on wetting and tends to slake, like a fragipan does. In thin section, the material appears as a matrix of amorphous isotropic glass containing angular pyroclasts of lava (lapilli, 20–50 μm across) and with phenocrysts of feldspars and quartz (Creutzberg *et al*., 1990), and it is similar to the tepetates in Mexico described by Oleschko (1990) and Hidalgo *et al*. (1995). It is porous but most of the

Correspondence: P. Podwojewski. E-mail: podwo@bondy.ird.fr
Received 10 December 2002; revised version accepted 14 October 2003

Figure 1 Outcrop of bare surface of cangahua, 2800 m above sea level, El Angel (Carchi Province, Ecuador). The raised mounts covered by vegetation are recent Holocene ash deposits preserved from erosion.

Figure 2 Surface of a hardened layer of cangahua with a millimetric structure.

pores are closed vesicles up to 200 μm in diameter. It contains some fine fissures resulting from shrinkage. This structure does not readily transmit water, which therefore runs off when it rains heavily, leading to erosion.

We have studied the cangahua in the inter-Cordillera valley of Ecuador (see Figure 4) where attempts are being made to use the land for agriculture. As above, the human population is growing in the region. The current density is between 100 and 150 inhabitants per square kilometre, and it is increasing 1.5–2% per year (Huttel *et al.*, 1999). Since the agrarian reforms of 1964 and 1974 small-holders have extended their cultivation on to the cangahua. This has caused loss of the loose topsoil, so that the hard cangahua is now at the surface and the land is sterile (De Noni *et al.*, 2001). To bring the land back into production the hard layers are broken up by machines with teeth 60 cm deep. This procedure creates large blocks which are then further fragmented by ploughing. The result is a material into which crops can be sown but which is almost totally lacking in organic matter ($< 0.1\%$) and deficient in nitrogen (N), phosphorus (P) and sulphur (S) for plant growth. With fertilizer N at 80–120 kg ha^{-1} and 60 kg P ha^{-1} the cangahua will produce crops, giving yields of maize of

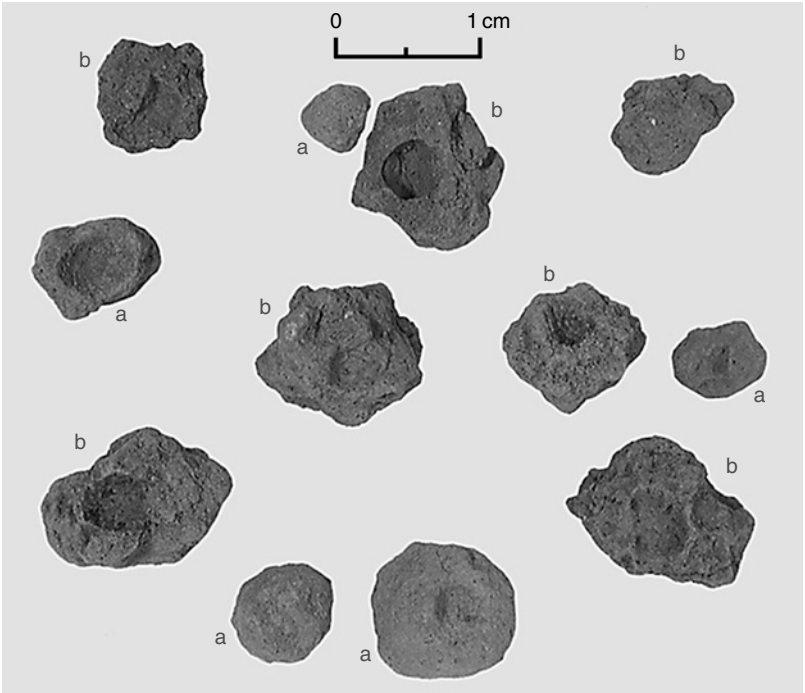

Figure 3 Morphology of particles resulting from the fragmentation of the cangahua in La Tola: a, rounded particles: accretionary lapilli; b, angular fragments with concavities: former muddy matrix of fine ashes including the lapilli.

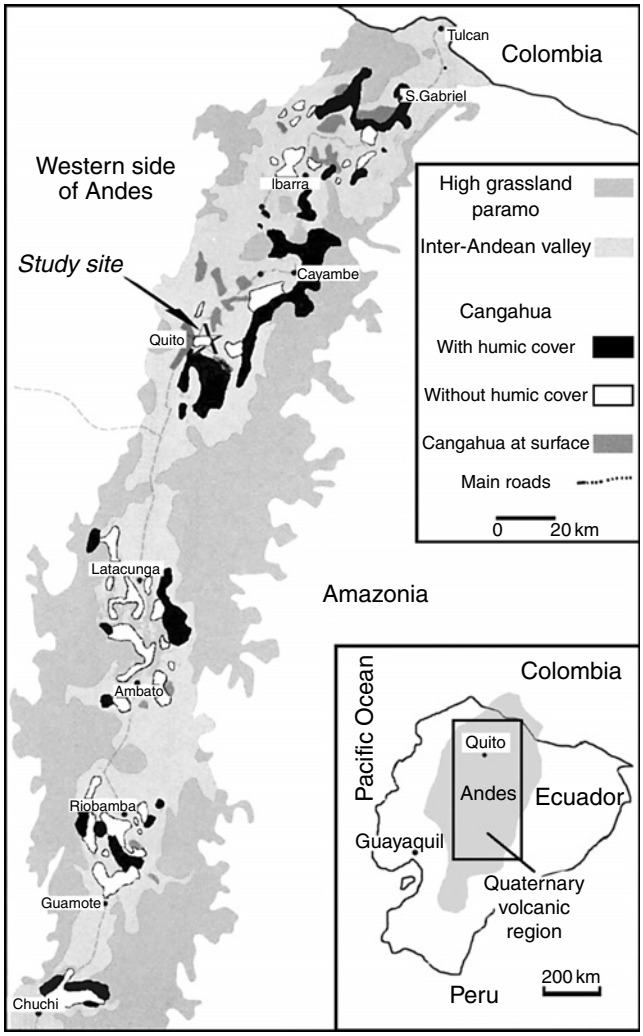

Figure 4 Location of study site and the occurrence of cangahua in central Ecuador.

more than 2 t ha^{-1} (Zebrowski, 1997), and with 800 kg N ha^{-1}, 100 kg P ha^{-1} and 50 kg S ha^{-1} it will produce more than 25 t ryegrass (*Lolium perenne*) per year. Nevertheless, the new soil is still prone to erosion, and De Noni *et al.* (2001) recorded losses of 100 t ha^{-1}.

Managing the cangahua and controlling erosion depends on maintaining an open structure. We have therefore been studying the way in which the structure evolves under cultivation in various farming regimes.

We compared plots with (i) different soil preparation (coarse or fine fragments), (ii) different inputs of organic matter, which were intended to improve soil structural stability (Tisdall & Oades, 1982; Perfect & Kay, 1989; Haynes *et al.*, 1991), and (iii) pasture with small amounts of fertilizers producing small yields as opposed to pasture receiving large amounts of fertilizers producing large yields with mycelium production, and large root densities which are also considered to improve the soil structural stability (Reid & Goss, 1993; Traoré *et al.*, 2000).

Materials and methods

The study and experimental design

The study was done on the experimental farm of the Faculty of Agronomic Science of the Central University of Ecuador. The farm is near the city of Tumbaco, near the Ilaló volcano, 20 km east of Quito at an altitude of 2465 m. The cangahua there is representative of the layers described by Winckell & Zebrowski (1992).

The annual average rainfall is 800 mm, and there are two rainy seasons. The main season is from January to June, and the minor one from October to November or December. The monthly average temperature is 15.7°C with little annual variation. The relative air humidity is 75%, and there are more than 2000 hours of insolation per year.

The grain-size distribution was measured in three plots at several depths before the experiment. It was fairly homogeneous across the site with a bimodal distribution of large amounts of fine sands and fine silts (Table 1). The bulk density of this hard material is 1.5 kg dm^{-3} with a porosity of 40%.

The chemical properties of the cangahua at La Tola determined in several specific studies and synthesized by Quantin & Zebrowski (1997) and De Noni *et al.* (2001) are listed in Table 2. It has a neutral pH in the range 6.5–7.5 in the presence of carbonates, and a large proportion of exchangeable cations which are well balanced. However, its organic matter content is very small, and the material is very deficient in N and P.

The experimental plots and subplots

Five levels of the cangahua with a step of 1 m high were chiselled to a depth of 60 cm with a bulldozer and levelled into five flat terraces 6 m wide × 50 m long. The rootable soil did not exceed 40 cm in depth. Each terrace comprised two plots (Figure 5), with a general slope $< 1\%$ oriented to the west. Each plot had an area of approximately 100 m^2 (4.5 m × 22 m). Initially, the cangahua on five of the plots was fragmented into coarse fragments (c) and five into fine fragments (f). Coarse fragments (20 cm in diameter) resulted from a one-way drag of a bulldozer tooth every 2 m lengthwise across the terrace. Finer fragments (F) (< 10 cm in diameter) resulted

Table 1 Grain-size distribution in three plots of the La Tola site

		Grain-size distribution /%				
Plot	Depth /cm	CS	FS	CSi	FSi	C
1. WFc	0–5	20.7	30.4	9.8	32.7	6.4
6. GREENf	5–15	23.7	27.4	5.4	34.2	9.3
9. NPKf	15–25	34.5	27.5	7.1	22.9	7.9

CS, coarse sand 2000–200 μm; FS, fine sand 200–50 μm; CSi, coarse silt 50–20 μm; FSi, fine silt 20–2 μm; C, clay < 2 μm.

Table 2 Main chemical properties of the surface horizon (0–10 cm) at the La Tola site

Exchangeable cations /cmol(+) kg^{-1}					Organic matter /g kg^{-1}				pH	
Ca^{2+}	Mg^{2+}	K^{+}	Na^{+}	CEC	C	N	C/N	P /mg kg^{-1}	in water	in KCl
7.9	5.5	0.7	0.4	18.8	4.1	0.54	7.6	457	6.85	5.20

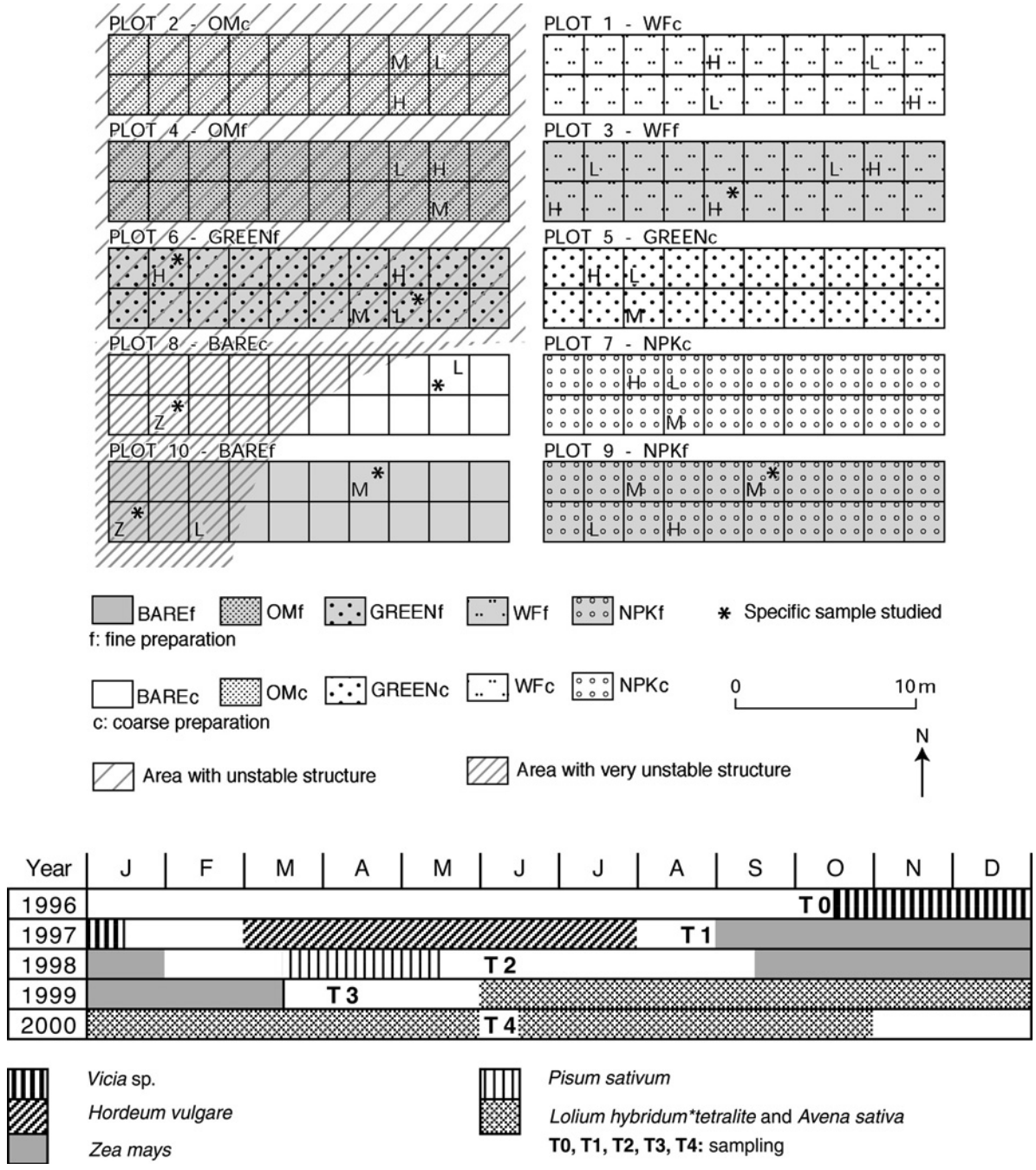

Figure 5 Location of the field plots, and the sampling and cultivation calendar.

from a one-way drag at 1-m intervals followed by preparation with a disc plough. Five different management treatments were applied on both sizes of cangahua fragmentation during the five cycles of cultivation (Figure 5). They were as follows.

1 OM: organic matter plots, with an incorporation of fresh cattle manure representing 40 t ha^{-1} of dry material before the first cultivation and a complement of 10 t ha^{-1} after each cultivation cycle representing a total amount exceeding 80 t ha^{-1}.

2 GREEN: green manure (all the residues of previous cultivation were buried), total of 10 t ha^{-1} including 6 t ha^{-1} of *Vicia* sp. and 2 t ha^{-1} of *Pisum sativum* (peas), and chemical fertilizers as a complement.

3 NP: initial mineral fertilization 300 kg N ha^{-1}; 80 kg P ha^{-1} with a complement of 50 kg N ha^{-1} and of 10 kg P ha^{-1} after each cycle.

4 WF: cultivation without fertilizers.

5 BARE: plots maintained bare and uncultivated.

Samples were collected at four different stages of cultivation (Figure 5), as follows.

1 T0: after the fragmentation of the rock, before cultivation.

2 T1: after 3 years of cultivation, one cycle of *Vicia* sp. and a cycle of barley (*Hordeum vulgare*).

3 T2: after 2 years of cultivation, an aborted cycle of maize (*Zea mays*), and a short cycle of peas.

4 T3: after 3 years of cultivation and a cycle of maize.

After 3 years of cultivation (T3), each plot was divided into 20 subplots for a cycle of perennial cultivation of *Lolium hybridum* var. *tetralite* (ryegrass) or a cycle of oats (*Avena sativa*). Three fertilization treatments were applied on each plot, with one treatment per subplot: L (low), 60 kg N; M (medium), 280 kg N; H (high), 960 kg N and 60 kg P.

5 T4: after 4 years of cultivation: the last sampling was made after nine grass cuts; each cut was made at 5-week intervals.

Analytical methods

Measurement of soil aggregate stability. Samples were collected from the surface horizon in cores 6 cm in diameter and 10 cm deep in each plot with three replicates dispersed randomly in the plot. After 1 year (T1) and two cultivation cycles, we determined the contents in macroaggregates by sieving the samples in cold and warm water with a 0.2-mm sieve at the IRD laboratory in Montpellier. This method (Barthès *et al.*, 1996) was adapted from Kemper & Rosenau (1986): soil aggregates are rapidly immersed into deionized water for 2 hours, and then wet-sieved. The same test was carried out by immersion in warm water (2 hours in total with 1 hour at 95°C).

After 2 years (T2) and four cultivation cycles, the samples were sieved with six sieves under dry conditions, and then sieved again immersed in cold water. This method was also inspired by Kemper & Rosenau (1986). Aggregates in 100 g air-dried samples were graded by rotary sieving for 3 minutes through six sieves (250, 500, 1000, 2000, 4500 and 9700 μm) to determine seven classes of aggregates (Kemper & Rosenau, 1986). Subsequently, the same fraction was immersed for 2 hours in water and sieved under water with the same seven sieves.

After 3 years' cultivation (T3 and T4), the aggregate stability was measured by a simplified method: 20 g of 1–2 mm fraction sample was sieved under dry conditions, then sieved under water after immersion. We chose a 1-mm sieve to discriminate macro- and microaggregates instead of using the 250 μm usually adopted (Tisdall & Oades, 1982; Barthès *et al.*, 1996), because the latter corresponds to the fine sand fraction, which composes almost one third of the mass of the soils we studied.

The percentage of water-stable aggregate is

$$W = 100 \times P_s/P_w,$$

where P_s is the weight of soil on the sieve after sieving in water then oven-dried and weighed and P_w is the weight of the initial soil sample. The per cent of unstable wet aggregates (U) is $100 - W$.

At stage T4 measurements of unstable wet aggregates of 1–2 mm in size of the plots 2, 4, 5, 6, 7 and 9 were analysed by an analysis of variance, appropriate to a factorial design, with six replicates and with the initial mechanical removal (Coarse, Fine) and the accumulated biomass of ryegrass (Low, Medium, High) as the two main factors. An additional analysis of variance was also made, with a factorial design with six replicates and the plot (P2, P4, P5, P6, P7, P9) as the main factor.

Additional analyses. Complementary analyses were made once we had the results of the aggregate stability measurements at eight locations, which showed the most dispersive values (Figure 5). Selective extractions of aluminium (Al), iron (Fe) and silica (Si) were made with 0.2 M ammonium oxalate (ox) at pH 3 (soil/solution ratio 1/40), and with citrate–dithionite–bicarbonate (cdb). The Al, Fe and Si of all extracts were measured by ICP-AES spectrophotometer at the IRD laboratory in Bondy, France. The grain-size distribution was determined on 10 g of soil after destruction of organic matter, with hexametaphosphate and 30 minutes' ultrasonic dispersion. We determined the sandy fractions (0.05–0.02 mm and 0.02–2 mm) by sieving the material under water. The coarse silt (0.02–0.05 mm), fine silt (0.002–0.02 mm) and clay (< 0.002 mm) fractions were determined with an X-ray sedigraph at the IRD laboratory at Bondy. The bulk density of the hard cangahua fragments was determined by the paraffin method on five replicates.

Among these eight specific samples, mineralogical determinations were made on two samples in plots 9 and 10 at the same terrace showing the most extreme behaviour. Mineralogical composition was determined by particle X-ray diffraction (XRD) with CuK radiation. Soil fragments were studied with a Cambridge STEREOSCAN 200 scanning electron microscope (SEM) coupled with a LEO AN 10 000 energy dispersive spectrometer (EDS). The shrinkage curves are made with a laser telemeter by the method of Braudeau *et al.* (1999).

Results

Variability of the soil structure

Before cultivation (T0), on wet sieving, the coarse preparation (c) produced more fragments > 1 mm or 250 μm than the fine preparation (f) with a lower variation coefficient for the fine aggregates (Table 3).

After 1 year of cultivation (T1), no effect of soil preparation could be observed. There were no significant differences in the content of macroaggregates among plots (Table 4). Nor was there any difference between using cold or hot water, which permits the dissolution of polysaccharides responsible for aggregation (Haynes *et al*., 1991; Barthès *et al*., 1996).

After 2 years' cultivation (T2), unstable wet aggregates (UWA) were mainly very coarse fragments which under wet sieving are largely responsible for the increase of fragments < 250 μm (Figure 6). The results show that there is apparently no relation between structural stability and organic fertilizer inputs. Plots 2, 6 and 8 showed the greatest UWA.

After 3 years' cultivation (T3), the percentage of unstable wet aggregates increased significantly. Plots on which the structure was unstable at T2 also had unstable structure at T3. In addition plots 4 and 10 also became unstable. All these plots with even numbers are in the western part of the experiment (Figure 7).

After 4 years' cultivation (T4), we observed the same behaviour for each of the plots as at T3. The proportions of unstable wet 1–2 mm aggregates and 2–4.7 mm aggregates are closely correlated ($r = 0.98$, $n = 33$). Plots with a dry matter production of 3 t ha^{-1} on the same terrace were not significantly different in structural stability from ones producing more than 20 t ha^{-1}. The amount of accumulated aboveground biomass of ryegrass did not influence the structural stability significantly in a one-year ryegrass treatment (Table 5, Table 7).

Table 3 Average of weight percentages and standard errors of fragments > 250 and > 1000 μm after wet sieving, for fine and coarse plots at T0

Average	Fine preparation (f)	Coarse preparation (c)
Fragments > 250 μm	67.6 ± 4.7	75.2 ± 5.3
Fragments > 1000 μm	47.6 ± 5.7	55.9 ± 6.7

Table 4 Proportions (as percentage and their standard errors) of macroaggregates > 250 μm in cold and hot water at T1

Plot	Cold water	Hot water
1. WFc	35.5 ± 3.2	28.4 ± 2.5
2. OMc	41.9 ± 3.3	44.6 ± 1.5
3. WFf	28.3 ± 2.6	
4. OMf	31.6 ± 5.4	33.3 ± 1.4
5. GREENc	31.3 ± 4.5	34.9 ± 0.7
6. GREENf	40.7 ± 2.2	40.2 ± 2.4
7. NPKc	33.3 ± 5.2	31.6 ± 2.9
8. BAREc	36.2 ± 2.1	35.7 ± 2.9
9. NPKf	36.3 ± 2.4	37.4 ± 1.6
10. BAREf	45.6 ± 4.3	39.4 ± 1.1

The soil components

Structural stability was highly variable on the plots in the western part of the trial. The aggregates there were less stable than on the eastern parts. For these reasons, we selected eight representative samples on both parts for further chemical and mineralogical analysis.

Chemical and physical properties. After introduction of cattle manure in each cycle, OM and GREEN plots had organic carbon contents of ≈ 7 g kg^{-1} or greater, whereas the plots WF without organic matter inputs had carbon contents of only 3 g kg^{-1} (Table 6).

After 3 years of cultivation, there was a clear difference in the grain-size composition of the soil surface. Compared with the initial grain-size composition (Table 1), in all plots, the coarse sand content decreased strongly and, conversely, the clay-size fraction and also the coarse silt fraction content increased. In the eastern part of the trial, plots were composed of homogeneous material poor in clay, while the extreme western part showed an increase in clay content (Table 7).

Mineralogy and micromorphology. The X-ray determinations of the oriented clay fraction showed no well-defined crystalline clays. However, a base line with an apparent greater intensity between 1 and 1.5 nm appears for samples with a larger content of clay-sized material (Figure 8). Nevertheless, this clear difference cannot be interpreted as a difference of clay type or of clay crystallinity.

The SEM images showed a differentiation between samples rich in clay and those containing little clay collected on the same plot. The latter contained homometric 10-μm angular grains with much intergranular porosity, whereas a clay-rich sample had isolated angular 10-μm grains and also more extended continuous planar areas (right side of Figure 9).

Discussion

The analysis of variance made at stage T4 shows that soil preparation, and grass root and mucilage production, had no significant effect on structural stability; only the sampling location on plots with different mineralogical properties had a significant influence (Table 8).

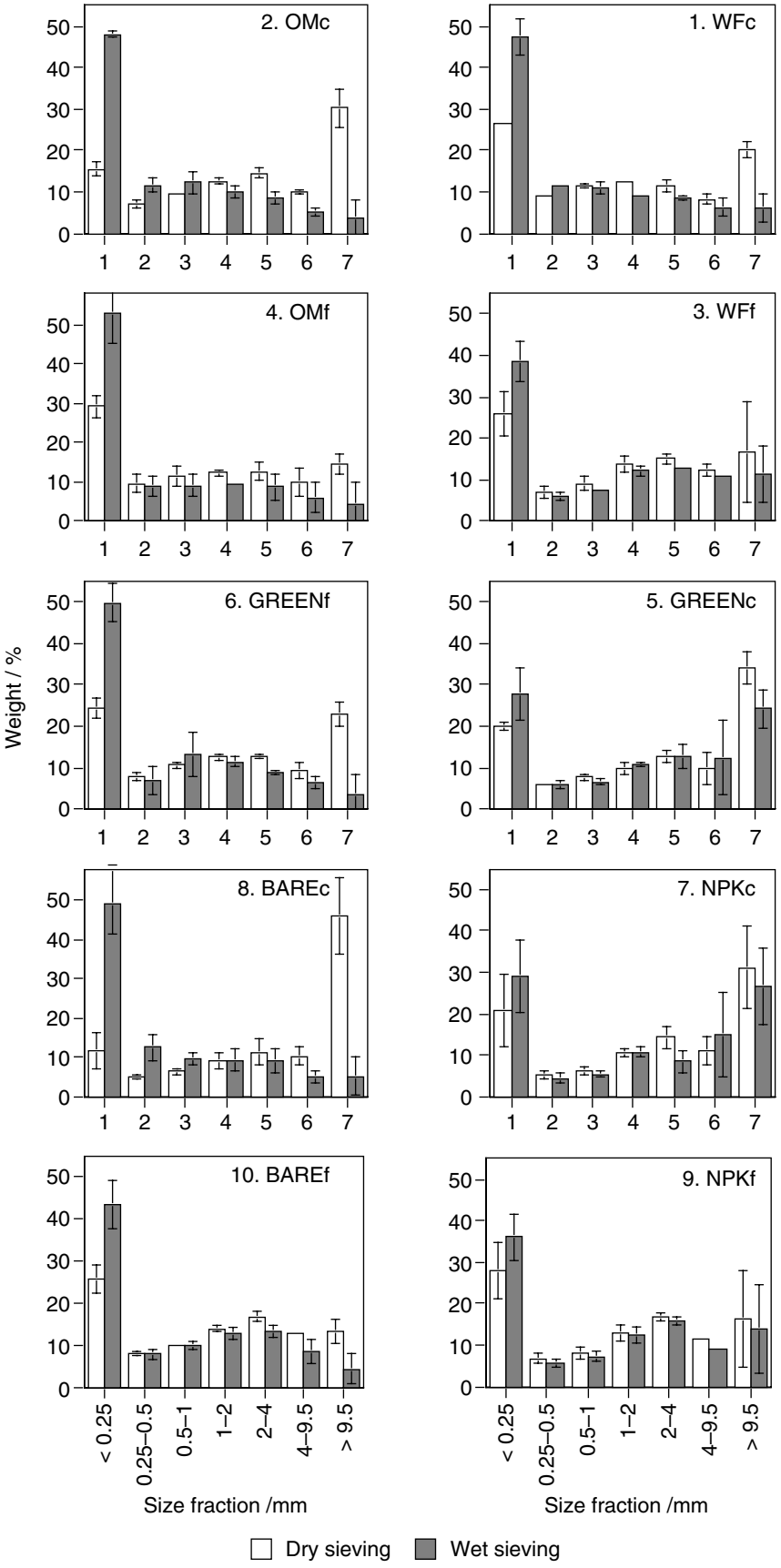

Figure 6 Weight percentage (with standard deviation) of different classes of aggregates in dry then in wet conditions after T2.

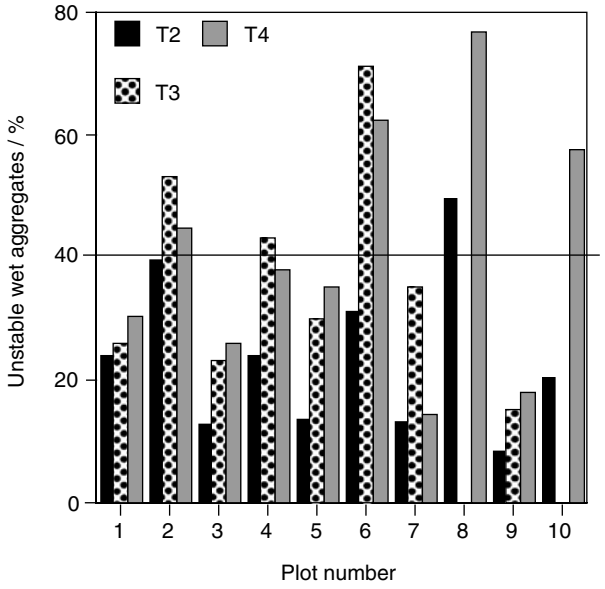

Figure 7 Unstable wet aggregates index of the plots after T2, T3 and T4.

Structural stability and carbon content

The formation of a typical soil structure and its stability are generally linked to carbon content (Tisdall & Oades, 1982). We think that the organic matter production derived from root degradation, the production of root exudates from perennial grass cover, and the development of a complete soil cover by mycelium observed in our high-yield plots had a strong positive effect on structural stability, in accord with the findings of Haynes & Swift (1990), Reid & Goss (1993) and Traoré *et al*. (2000). In the case of cangahua, in the early stages of agricultural management, fragments have a structure that is independent of surface mycelium, roots or carbon content.

For a positive effect on structural stability, the content of organic matter should exceed 2% in temperate climates (Greenland *et al*., 1975). In our experiment the concentration of organic matter was less than 2% except on plots receiving the most organic matter. Even after inputs of more than 80 t ha^{-1} of manure the cangahua contained less organic matter than degraded Ecuadorian soils on other types of parent rock (Harden, 1996). It seems that the lack of carbon in the cangahua after addition of so much organic matter is due to rapid mineralization. In similar soils in Mexico, after 4 months, more than a third of the input was mineralized (Etchevers *et al*., 1997).

Structural stability and clay content

The lack of crystalline clay minerals means that there are few bonds between clay and organic matter to form stable aggregates (Emerson, 1983). But in the case of cangahua we observed that an increase in the content of clay-size particles corresponds to an increase in the proportion of unstable aggregates ($r = 0.93$) and the aggregate stability might be related to iron oxide bonds ($r = 0.76$; Figure 10), as suggested by Emerson (1983). This unstable behaviour could be linked to the swelling and shrinking properties of the clay. The clay-rich fragments shrink by 5–8% after drying, whereas the clay-poor ones shrink by less than 1% (Figure 11). This behaviour confirms the presence of material with some capacity to swell in the clay-rich samples and could be responsible for the slaking of the fragments.

The studies of Creutzberg *et al*. (1990) and Hidalgo *et al*. (1995) on tepetates in Mexico showed a coating by a material

Table 5 Percentages of unstable wet aggregates (UWA) in the surface horizon (0–10 cm) in relation to fertilizer inputs, and ryegrass yield during the last cultivation cycle at stage T4

Plot	UWA 1–2	UWA 2–4.7	Yield /t ha^{-1}
1Ha	47.3	39.4	17.9
1Hb	27.1	25.8	12.7
1La	23.1	22.5	2.2
1Lb	15.6	11.2	2.4
3Ha	30.6	27.5	16.6
3Hb	42.9	37.1	16.0
3La	39.1	35.7	3.7
3Lb	9.2	6.0	2.6
2H	*51.5*	*51.9*	*21.8*
2M	*44.2*	*47.0*	*18.3*
2L	*44.3*	*48.1*	*6.1*
4H	*49.8*	*45.4*	*26.1*
4M	32.2	37.1	15.6
4L	25.0	18.6	9.0
5H	44.4	39.2	17.5
5M	41.3	30.1	11.8
5L	36.3	31.1	5.9
6H	*54.0*	*47.5*	*22.4*
6M	*58.5*	*50.6*	*14.4*
6L	*66.9*	*68.3*	*4.6*
7H	18.9		13.9
7M	13.4		13.0
7L	12.9		6.7
9H	9.0	7.1	20.1
9M	14.9		12.7
9L	33.0	31.0	8.0
8Z	*64.2*	*65.8*	*0.0*
10M	19.5	15.1	2.0
10L	*63.1*	*73.0*	*0.3*
10Z	*85.8*	*90.8*	*0.0*

Fertilizer inputs for ryegrass only: H, high; M, medium; L, low. Z, not cultivated.
UWA 1–2: % unstable wet aggregates (g 100 g^{-1}) 1–2 mm in size; UWA 2–4.7: % 2–4.7 mm in size.
Unstable aggregates plots (both values > 45%) are in italic.

Table 6 Carbon content (in g kg^{-1}) in the surface horizon (0–10 cm) during the experiment. The samples were collected before fertilizers were added

Plot	T0	T0.5	T1	T2	T3	T4
1. WFc	2.6	4.3	4.7	1.6	3.7	3.7
2. OMc	3.1	16.7	12.1	6.8	9.6	7.8
3. WFf	2.0	4.3	4.7	1.6	1.6	2.6
4. OMf	2.4	16.3	11.1	7.4	12.6	7.4
5. GREENc	1.8	7.6	11.2	2.7	12.1	6.2
6. GREENf	4.3	5.4	11.0	3.3	9.3	7.3
7. NPKc	2.6	6.4	5.3	2.7	7.2	3.0
8. BAREc	1.6			1.6		
9. NPKf	1.2	5.1	5.0	2.4	6.5	2.7
10. BAREf	2.2			2.2		

rich in amorphous silica. Air-dried samples did not slake after prolonged immersion in water. However, a mechanical disruption of this coating allowed water to enter the aggregates. Subsequently the soil material was easily dispersed (Creutzberg *et al.*, 1990). In the cangahua of Ecuador, the amounts of amorphous silica ($<1\%$ for citrate–bicarbonate–dithionite extract and $<0.1\%$ for oxalate extract, Table 6) are too small to explain any allophane or amorphous silica bonds or coatings like those described by Jongmans *et al.* (2000). But the disruption of the impermeable layers of cangahua allowed the isolated fragments to swell and shrink. Exposure to rain and the effects of tillage might have caused the fragments to split and so produce coarse sand-sized aggregates of finer particles, and this process might explain the increase of the fine fraction during the trial. In our case, iron oxides were probably more important agents for the particle cohesion than amorphous silica (Figure 10) and explain the difference in structural stability of the samples.

Table 7 Physical and chemical data of selected samples. Plots at the extreme west of the trial (even numbers) with the least stable soil are in italic

Sample	3H	6L	*6H*	8L	*8Z*	9M	10M	*10Z*
Particle size								
Coarse sand /%	12.1	8.6	*6.8*	7.8	*11.5*	12.1	9.6	*10.3*
Fine sand /%	30.3	32.7	*26.8*	31.0	*41.2*	36.5	36.7	*36.1*
Coarse silt /%	16.9	13.7	*12.2*	13.6	*7.2*	12.5	12.5	*10.2*
Fine silt /%	32.5	32.6	*30.4*	32.4	*15.6*	27.9	24.7	*22.0*
Clay /%	7.1	10.9	*18.2*	14.5	*22.3*	8.6	10.6	*18.9*
Oxalate extractable								
Al_{ox} /g kg^{-1}	1.34	1.41	*1.40*	1.30	*1.05*	1.29	1.25	*1.24*
Fe_{ox} /g kg^{-1}	1.91	1.87	*1.70*	1.49	*2.31*	1.55	1.72	*2.44*
Si_{ox} /g kg^{-1}	0.61	0.65	*0.64*	0.57	*0.51*	0.56	0.56	*0.56*
CBD extractable								
Al_{cbd} /g kg^{-1}	1.73	1.71	*1.79*	1.73	*1.51*	1.96	1.70	*1.95*
Fe_{cbd} /g kg^{-1}	11.19	9.93	*10.61*	10.68	*7.01*	11.42	10.61	*8.93*
Si_{cbd} /g kg^{-1}	7.39	6.76	*7.48*	6.95	*4.43*	8.23	7.05	*6.21*
$(Al + 1/2\ Fe)_{ox}$ /%	0.23	0.23	*0.23*	0.20	*0.22*	0.21	0.21	*0.25*

The natural cangahua exposed to rain is fairly resistant to erosion, but once disturbed, the cangahua shows an irregular pattern of erosion linked to the local variation of mineralogy and weathering stage of the cangahua. Such lateral variations were also observed by J. Bertaux (personal communication) for the weathering of some tepetates in Mexico.

Agronomic consequences

Massive quantities of organic matter are likely to be required to create stable aggregates. They are not available locally, and importing them would be too costly. Any tillage would break the fragments and increase the sensitivity to erosion. Therefore the best form of agricultural development on the cangahua might be perennial grass (Kay, 1990). The fibrous roots of the grasses not only ramify and open up the soil but also encompass individual crumbs in a net-like web to form clusters resistant to slaking. Trampling by livestock would break the fragments of cangahua and compact the surface, again making the land susceptible to erosion. So the herbage should be cut and carried to the animals rather than grazed.

Conclusion

The cangahua is a geological formation which can be fragmented by deep cultivation to produce a 'soil' in which crops can be grown. In time these fragments will disintegrate into elementary particles. After 4 years of cultivation, the soil preparation, organic matter inputs, root density or mucilage production had no effect on the stability of the structure. The early stability of fragments is determined by the mineralogical composition: clay-rich material which shrinks and swells is less stable than material containing little clay, with less shrink–swell properties and containing more Fe_{cbd}. These different stages of weathering generate irregularities in the erosion process.

The best form of agriculture on the cangahua might be perennial grass with a complete soil cover limiting the erosion and with a probable long-term positive effect on structural stability.

Acknowledgements

This paper is dedicated to our two friends from IRD: Claude Zebrowski who initiated the agronomic study and died during the trial in 1998 and Jacques Bertaux, mineralogist, who left us in 2002 after working on cangahua and tepetates for several

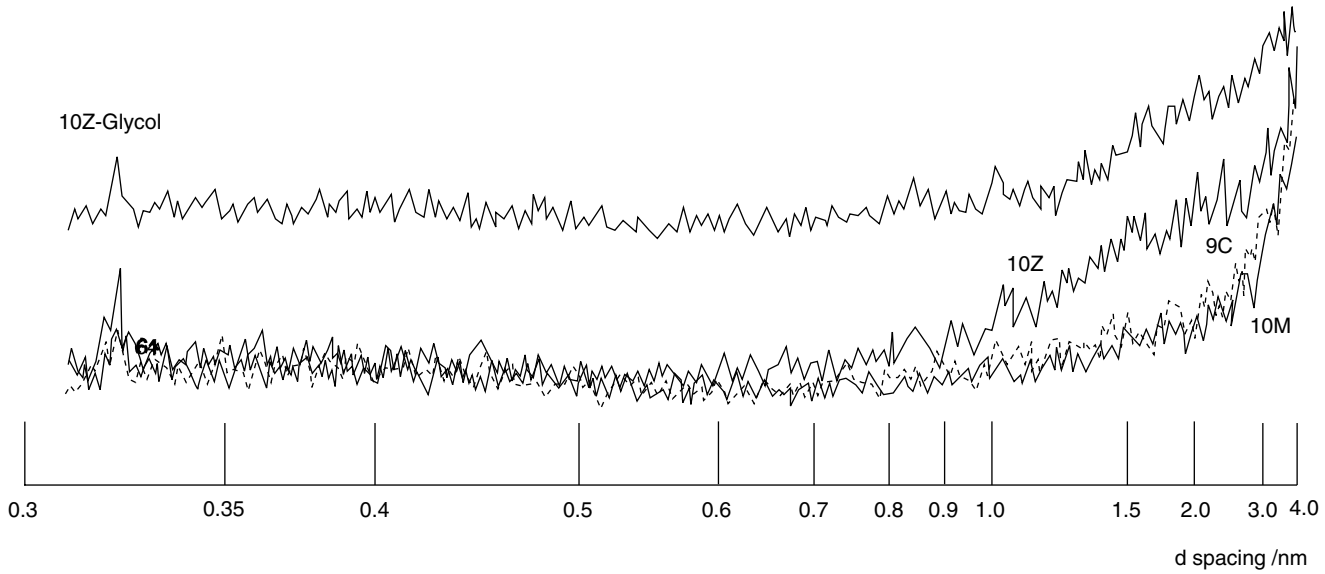

Figure 8 X-ray diffraction patterns: oriented clays on clay-poor (plots 9M and 10M) and clay-rich (plot 10Z) fragments; glycol treatment on plot 10Z.

Table 8 Effect of initial mechanical removal (IMR), accumulated above-ground biomass of ryegrass (AABR) and subplot location on unstable wet aggregates (UWA) 1–2 mm (%) at T4. Analysis of variance (ANOVA)

Factor	Level	UWA	ANOVA
IMR	Coarse	31.2 (14.5)	NS
	Fine	39.2 (20.1)	
AABR	Low	36.8 (19.0)	NS
	Medium	34.5 (17.2)	
	High	34.4 (17.1)	
Interaction	Coarse × Low	30.0 (17.7)	NS
IMR × AABR	Coarse × Medium	30.8 (15.1)	
	Coarse × High	33.0 (13.4)	
	Fine × Low	43.6 (22.0)	
	Fine × Medium	38.3 (20.6)	
	Fine × High	35.8 (21.5)	
Plot	P2	44.6 (8.2)	
	P4	37.7 (8.5)	
	P5	35.1 (7.6)	***
	P6	62.3 (7.9)	
	P7	14.1 (3.8)	
	P9	17.8 (9.0)	

NS, not significant; ***, significant at $P = 0.001$.
Per treatment means, with standard errors in parentheses.

years. We thank the Central University of Ecuador, the soil laboratory of CESA at Tumbaco, the staff of the IRD-CANGAHUA programme, the Editor and Christian Valentin for valuable comments on our script.

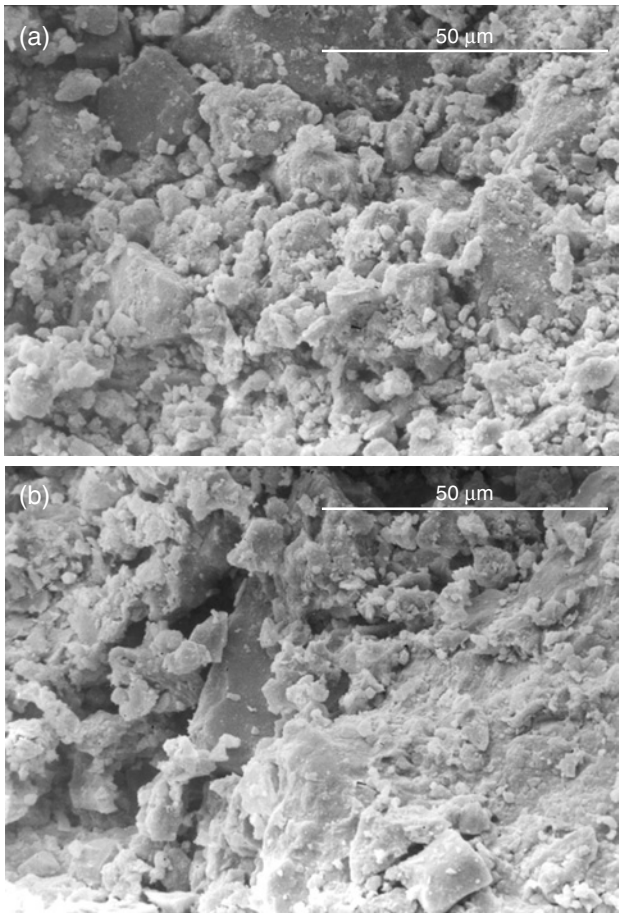

Figure 9 Scanning electron microscope view of (a) clay-poor (plot 9M) and (b) clay-rich (plot 10Z) fragments, with an extended planar area on the right of (b).

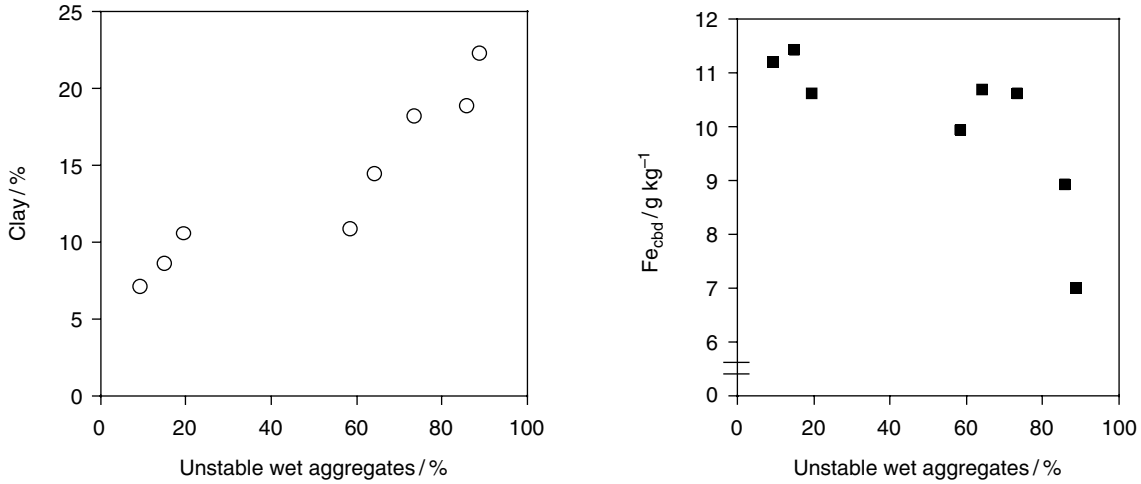

Figure 10 Relation between unstable wet aggregates and cangahua clay and Fe (citrate–bicarbonate–dithionite extract) contents.

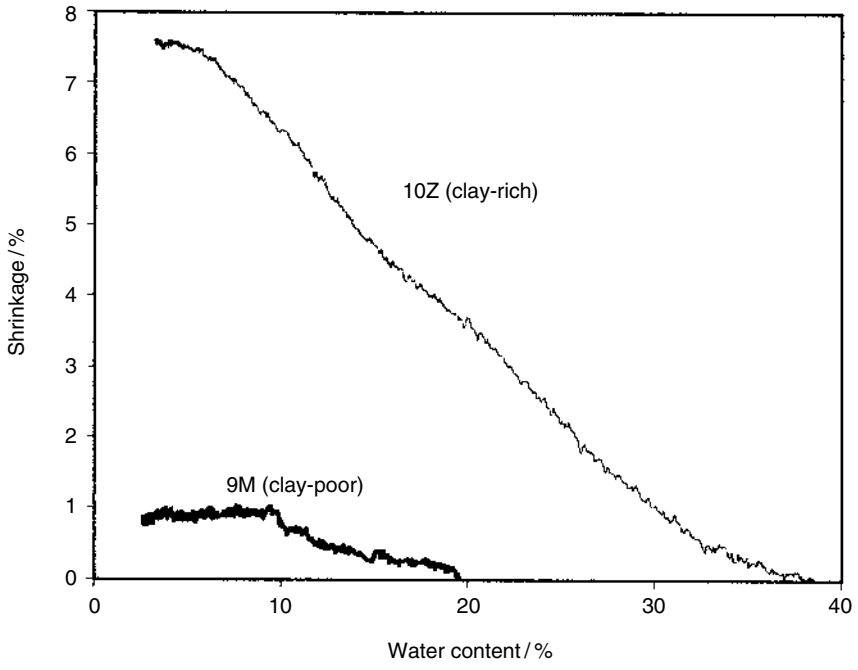

Figure 11 Shrinkage curves as a function of water content of clay-poor (plot 9M) and clay-rich (plot 10Z) fragments.

References

Barthès, B., Kouakoua, G., Sala, G.H., Hartmann, C. & Nyeté, B. 1996. Effet à court terme de la mise en culture sur le statut organique et l'agrégation d'un sol ferrallitique argileux du Congo. *Canadian Journal of Soil Science*, **76,** 493–499.

Braudeau, E., Constantini, J.M., Bellier, G. & Colleuille, H. 1999. New device and method for soil shrinkage curve measurement and characterization. *Soil Science Society of America Journal*, **63,** 525–535.

Creutzberg, D., Kauffman, J.H., Bridges, E.M. & Guillermo Del Posso, M. 1990. Micromorphology of 'Cangahua'. A cemented subsurface horizon in soils from Ecuador. In: *Soil Micromorphology: A Basic and Applied Science* (ed. L.A. Douglas), pp. 367–372. Developments in Soil Science 19, Elsevier, Amsterdam.

De Noni, G., Viennot, M., Asseline, J. & Trujillo, G. 2001. *Terres d'altitude, terres de risque. La lutte contre l'érosion dans les Andes équatoriennes.* Latitudes 23, IRD, Paris.

Emerson, W.W. 1983. Inter-particle bounding. In: *Soils: An Australian Viewpoint*, pp. 477–498. Division of Soils, CSIRO, Melbourne.

Etchevers, J.D., Pérez, M.A. & Navarro, G. 1997. Dinámica de la materia orgánica y el N en tepetates habilitados para la producción agrícola. In: *Memoria del III Simposio Internacional sobre Suelos Endurecidos (Quito, diciembre de 1996)* (eds C. Zebrowski, P. Quantin & G. Trujillo), pp. 213–224. IRD, PUCE, UCE, Quito.

Fischer, R.V. & Schmincke, H.U. 1984. *Pyroclastic Rocks*. Springer-Verlag, Berlin.

Greenland, D.J., Rimmer, D. & Payne, D. 1975. Determination of the structural stability class of English and Welsh soils, using a water coherence test. *Journal of Soil Science*, **26,** 294–303.

Harden, C. 1996. Interrelationships between land abandonment and land degradation: a case from the Ecuadorian Andes. *Mountain Research and Development*, **16,** 274–280.

Haynes, R.J. & Swift, R.S. 1990. Stability of soil aggregates in relation to organic constituents and soil water content. *Journal of Soil Science*, **41,** 73–83.

Haynes, R.J., Swift, R.S. & Stephen, R.C. 1991. Influence of mixed cropping rotations (pasture–arable) on organic matter content, water stable aggregation and clod porosity in a group of soils. *Soil and Tillage Research*, **19,** 77–87.

Hidalgo, C., Bertaux, J. & Quantin, P. 1995. Forms of silica in indurated volcanic soils of the Mexico Valley. In: *Clays Controlling the Environment* (eds G.J. Churchman, R.W. Fitzpatrick & R.A. Eggleton), pp. 487–493. Proceedings of the 10th International Clay Conference, CSIRO, Melbourne.

Huttel, C., Zebrowski, C. & Gondard, P. 1999. Paisajes agrarios del Ecuador. *Geografía Básica del Ecuador*, Tomo V, Vol. 2. IRD, IPGH, IFEA, IGM, PUCE, Quito.

Jongmans, A.G., Denaix, L., van Oort, F. & Nieuwenhuyse, A. 2000. Induration of C horizons by allophane and imogolite in Costa Rican volcanic soils. *Soil Science Society of America Journal*, **64,** 254–262.

Kay, B. 1990. Rates of change of soil structure under different cropping systems. *Advances in Soil Science*, **12,** 1–52.

Kemper, W.D. & Rosenau, R.C. 1986. Aggregate stability and size distribution. In: *Methods of Soil Analysis: Part 1, Physical and Mineralogical Methods*, 2nd edn (ed. A. Klute), pp. 425–442. Agronomy Monograph No 9, Book Series 5, Soil Science Society of America, Madison, WI.

Moore, J.G. & Peck, D.L. 1962. Accretionary lapilli in volcanic rocks of the western continental United States. *Journal of Geology*, **70,** 182–194.

Moore, J.G., Nakamura, K. & Alcaraz, A. 1966. The 1965 eruption of Taal Volcano. *Science*, **151,** 955–960.

Oleschko, K. 1990. Cementing agents morphology and its relation to the nature of Tepetates. In: *Soil Micromorphology: A Basic and Applied Science* (ed. L.A. Douglas), pp. 381–386. Developments in Soil Science 19, Elsevier, Amsterdam.

Perfect, E. & Kay, B.D. 1989. Relations between aggregate stability and organic components for a silt loam soil. *Canadian Journal of Soil Science*, **70,** 731–735.

Quantin, P. 1992. L'induration des matériaux volcaniques pyroclastiques en Amérique latine: Processus géologiques et pédologiques. *Terra*, **10,** 24–33.

Quantin, P. & Zebrowski, C. 1997. Analyse préliminaire (chimie, minéralogie, pétrographie de quelques types de cangahua). Los suelos con cangahua en el Ecuador. In: *Memoria del III Simposio Internacional sobre Suelos Endurecidos (Quito, diciembre de 1996)* (eds C. Zebrowski, P. Quantin & G. Trujillo), pp. 29–47. IRD, PUCE, UCE, Quito.

Reid, J.B. & Goss, M.J. 1993. Effect of living roots of different plant species on the aggregate stability of two arable soils. *Journal of Soil Science*, **32,** 521–541.

Tisdall, J.M. & Oades, J.M. 1982. Organic matter and water-stable aggregates in soils. *Journal of Soil Science*, **33,** 141–163.

Traoré, O., Groleau-Renaud, V., Plantureux, S., Tubeileh, A. & Bœuf-Tremblay, V. 2000. Effect of root mucilage and modelled root exudates on soil structure. *European Journal of Soil Science*, **51,** 575–581.

Winckell, A. & Zebrowski, C. 1992. La cangahua en Equateur: le contexte paléogéographique de sa formation. *Terra*, **10,** 107–112.

Zebrowski, C. 1997. Los suelos con cangahua en el Ecuador. In: *Memoria del III Simposio Internacional sobre Suelos Endurecidos (Quito, diciembre de 1996)* (eds C. Zebrowski, P. Quantin & G. Trujillo), pp. 128–137. IRD, PUCE, UCE, Quito.